THE JOURNAL OF BIOLOGICAL CHEMISTRY VOL. 284, NO. 13, pp. 8930–8939, March 27, 2009

A Novel Role for Embigin to Promote Sprouting of Motor Nerve Terminals at the Neuromuscular Junction*[S]

Received for publication, December 17, 2008, and in revised form, January 21, 2009 Published, JBC Papers in Press, January 21, 2009, DOI 10.1074/jbc.M809491200

Enzo Lain[‡], Soizic Carnejac[‡], Pascal Escher[‡], Marieangela C. Wilson[§], Terje Lømo[¶], Nadesan Gajendran[‡], and Hans Rudolf Brenner[‡1]

From the [‡]Institute of Physiology, Department of Biomedicine, University of Basel, Klingelbergstrasse 50, Basel 4056, Switzerland, the [§]Department of Biochemistry, University of Bristol, School of Medical Sciences, Bristol BS8 1TD, United Kingdom, and the [¶]Department of Physiology, University of Oslo, Blindern N-0317, Oslo, Norway

Adult skeletal muscle accepts ectopic innervation by foreign motor axons only after section of its own nerve, suggesting that the formation of new neuromuscular junctions is promoted by muscle denervation. With the aim to identify new proteins involved in neuromuscular junction formation we performed an mRNA differential display on innervated *versus* denervated adult rat muscles. We identified transcripts encoding embigin, a transmembrane protein of the immunoglobulin superfamily (IgSF) class of cell adhesion molecules to be strongly regulated by the state of innervation. In innervated muscle it is preferentially localized to neuromuscular junctions. Forced overexpression in innervated muscle of a full-length *embigin* transgene, but not of an *embigin* fragment lacking the intracellular domain, promotes nerve terminal sprouting and the formation of additional acetylcholine receptor clusters at synaptic sites without affecting terminal Schwann cell number or morphology, and it delays the retraction of terminal sprouts following re-innervation of denervated endplates. Conversely, knockdown of *embigin* by RNA interference in wild-type muscle accelerates terminal sprout retraction, both by itself and synergistically with deletion of neural cell adhesion molecule. These findings indicate that embigin enhances neural cell adhesion molecule-dependent neuromuscular adhesion and thereby modulates neuromuscular junction formation and plasticity.

At the developing neuromuscular junction the heparan sulfate proteoglycan agrin from motor nerves interacts with the receptor tyrosine kinase MuSK (muscle specific kinase) in the muscle fiber to orchestrate the differentiation of both presynaptic nerve terminals (1) and the postsynaptic apparatus (2). In adult muscle, sectioning an adult muscle's own nerve is an essential condition for transplanted foreign nerves to form new ectopic endplates in its extrasynaptic regions. This model system recapitulates essential aspects of embryonic NMJ formation (3). In light of these findings, muscle denervation may promote ectopic synapse formation by one or a combination of the following mechanisms: 1) by up-regulating the extrasynaptic expression of MuSK or of signaling components downstream of MuSK, thus increasing the responsiveness of the fibers to agrin (4), 2) by inducing the secretion of factors from muscle that may stimulate the secretion of agrin from motor neurites, and 3) by promoting neuron-muscle fiber adhesion, which may promote stable agrin-MuSK interaction required for synaptic differentiation (5). Adhesion could be mediated by agrin itself, anchored in the basel lamina and interacting with the neural cell adhesion molecule (NCAM)[2] in the surface of motor neurons (6–8), or by up-regulation of adhesion molecules in muscle and/or motor neurites. Cell adhesion molecules (CAMs) such as NCAM and N-cadherin have been implicated in motor neuron sprouting. NCAM-induced sprouting is thought to be induced via homophilic binding between NCAMs in the neural and the muscle surfaces, that in turn induces growth promoting mechanisms in the nerve process (9–11). Interestingly, both NCAM and N-cadherin are expressed in the surface of developing muscle with a spatiotemporal pattern that is consistent with a role in NMJ formation (12): expression is along the entire myotube surface; once NMJ formation has begun, it is reduced to persist only at the NMJ. Upon denervation it is up-regulated in parallel with MuSK, AChRs, and the increased susceptibility of the muscle to innervation. Comparable evidence supports the hypothesis that tenascin-C, a glycoprotein component of extracellular matrix, is involved in neuromuscular interactions related to those of NCAMs (12–14). However, it has been difficult to demonstrate the importance of these molecules in vertebrate NMJ formation, because their ablation did not critically alter synapse formation (15) or was embryonically lethal (16). Combined these findings thus suggest that CAMs up-regulated by denervation are dispensable for early ectopic NMJ formation, that several nerve-muscle adhesion systems may be redundant, and/or that some may not have been identified.

Here we show that motor neurones constitutively overexpressing agrin and transplanted onto muscles constitutively overexpressing MuSK do not form ectopic synapses, unless the muscle's own nerve is sectioned, indicating that in addition

* This work was supported by grants from the Swiss National Science Foundation, the Swiss Foundation for Research on Muscle Diseases, and by the Kanton Basel-Stadt. The costs of publication of this article were defrayed in part by the payment of page charges. This article must therefore be hereby marked "*advertisement*" in accordance with 18 U.S.C. Section 1734 solely to indicate this fact.

[S] The on-line version of this article (available at http://www.jbc.org) contains supplemental Tables S1 and S2.

[1] To whom correspondence should be addressed. Tel.: 41-61-267-1638; Fax: 41-61-267-1628; E-mail: Hans-Rudolf.Brenner@unibas.ch.

[2] The abbreviations used are: NCAM, neural cell adhesion molecule; CAM, cell adhesion molecule; NMJ, neuromuscular junction; AChR, acetylcholine receptor; RT, reverse transcription; qRT, quantitative RT; RL8, ribosomal protein L8; MCK, muscle creatine kinase; MuSK, muscle specific kinase; wt, wild type; RNAi, RNA interference; shRNA, short hairpin RNA; GFP, green fluorescent protein.

to agrin/MuSK other denervation-induced interactions are required. Given that NCAM and tenascin-C expression in muscle are up-regulated by denervation (12, 13), yet their deletion does not seriously affect NMJ formation (15), we searched for new factors affecting neuromuscular interactions by screening mRNAs differentially expressed by innervated and chronically denervated muscle. We identified the IgS molecule embigin (17) in the muscle surface to be strongly regulated by electrical muscle activity and to exhibit functional properties consistent with a role in the outgrowth of motor neurons and the formation of NMJs.

EXPERIMENTAL PROCEDURES

Animals and Surgery

Rat soleus muscles of 7-week-old Wistar rats (weight of ~200 g) and mouse gastrocnemius muscles of 6-week-old C57/BL6 mice were denervated by cutting or crushing the sciatic nerve just proximally to its branching into tibial and fibular nerves. Ectopic endplates were induced in mice as described by (17). Rats and mice were killed with CO_2 at the post-denervation times indicated, and muscles were excised for analysis. In some experiments, denervated rat soleus muscles were stimulated chronically via implanted electrodes as previously described (18). For control samples, muscles were isolated from age-matched animals (innervated samples). Animal handling, surgery, and anesthesia were approved by the Cantonal Veterinary Office of Basel-Stadt.

RNA Preparation

For RNA extraction, dissected tissues were transferred into green-capped FastPrep™ tubes containing lysing matrix D (Bio101, Qbiogene) and filled with 1 ml of TRIReagent® (Molecular Research Products), then snap-frozen in liquid nitrogen and kept at −80 °C until homogenization. Tissues were homogenized by four 20-s shaking cycles on the FastPrep™ FP120 apparatus (Bio101, Qbiogene). RNA extraction was according to the manufacturer's instructions (Molecular Research Products).

mRNA Differential Display

For the initial mRNA differential display, total RNA from three of each nervated and 4-day-denervated rat soleus muscles was treated with DNase I (MessageClean®, GenHunter Corp.) before proceeding to mRNA differential display. We performed the mRNA differential display according to the manufacturer's protocol using RNAimage® kits containing H-AP primers 17–24 for mRNA differential display (GenHunter® Corp.), with the following modifications. PCR amplifications were performed in the presence of [α-^{33}P]dATP (PerkinElmer Life Sciences) in a final volume of 10 ml using AmpliTaq polymerase (Roche Applied Science). PCR amplification products were run on 6% polyacrylamide-urea sequencing gels and exposed to Kodak BioMax I films at −70 °C. Re-amplified PCR fragments were gel-purified with QIAEXII (Qiagen) and subcloned into pGEM®-T and pGEM®-T Easy vector systems (Promega, Madison, WI). Sequencing was performed on both strands on an ABI377 DNA Sequencer (Applied Biosystems). Sequences were identified through comparison to non-redundant public databases using the BLAST algorithm (www.ncbi.nlm.nih.gov/BLAST).

Northern Blot

Electrophoresis, blotting, hybridization, and washing were carried out according to the manufacturer's protocols (NorthernMax, Ambion) using positively charged nylon membranes (Roche Applied Science). We used as template for probe labeling full-length cDNA of mouse embigin (cloning see below). We subcloned a PCR-amplified 527-bp fragment of the mouse ribosomal protein L8 gene into pGEM-T easy vector (Invitrogen, primers 5′-ACTGGACAGTTCGTGTACTG-3′ and 5′-CTCTAGTTCTCCTTCTCCTG-3′). The resulting pRL8-527 vector was digested with EcoRI, and the gel-purified insert was used as template for probe synthesis. Radioactive probes were synthesized by random primed labeling (High Prime, Roche Molecular Biochemicals) with Redivue [α-^{32}P]dCTP (3000 Ci/mmol, Amersham Biosciences) and purified on mini Quick Spin DNA columns (Roche Molecular Biochemicals). Membranes were exposed on Kodak BioMax I films at −70 °C.

Quantitative PCR

Total RNA was treated with DNase I (Ambion) and reverse-transcribed with an oligo(dT) primer using the first strand cDNA synthesis kit for RT-PCR (avian myeloblastosis virus, Roche Applied Science). For quantitative PCR, cDNA was amplified with qPCR™ Mastermix Plus for SYBR® Green I (Eurogentec). Primer sequences used in PCR reactions were chosen based on the sequences available in public databases. Primers (Microsynth AG) were designed to generate a PCR amplification product of 160–220 bp spanning an intron on the genomic sequence. Only primer pairs yielding unique amplification products without primer dimer formation were subsequently used for real-time PCR assays. Quantitative PCR assays were performed on an ABI Prism 7000 Sequence Detection system (Applied Biosystems) using the manufacturer's amplification program. The mRNA expression of all assessed genes is normalized to ribosomal protein L8 (RL8) expression.

Western Blot and Immunocytochemistry

Rat soleus and mouse gastrocnemius muscles were transferred into 2-ml capped Sarstedt tubes containing 500 ml of lysis buffer (100 mM NaCl, 50 mM Tris, pH 7.5, 1 mM EDTA, 0.1% Triton X-100, 10 mM NaF, 1 mM vanadate, and proteinase inhibitors (Complete®, Roche Applied Science, Switzerland)) and 0.5 mm glassbeads (Glas Keller, Basel, Switzerland). Muscles were homogenized by four 20-s shaking cycles on the FastPrep™ FP120 apparatus (Bio101, Qbiogene). Homogenates were centrifuged at 4 °C for 10 min at 14,000 rpm, and supernatants were aliquoted and stored at −80 °C. For Western blot analysis, 80 mg of proteins was transferred by semi-dry blotting (Bio-Rad) on an Immobilon-P membrane (Millipore). Levels of full-length embigin protein were immunodetected with a purified rabbit polyclonal anti-embigin antibody (19). Because this antibody was raised against the intracellular domain of embigin, we used anti-Myc antibody to ascertain expression and

correct membrane insertion of Myc-tagged, truncated embigin ΔIC in Western blots and in transfected COS cells (Fig. 3*D*). A mouse monoclonal anti-β-tubulin antibody (Chemicon) was used to check for protein loading. AChRs were stained with α-bungarotoxin-Alexa594 (Invitrogen), Schwann cells were stained with anti-S-100 antibody (Z0311, DAKO). In some experiments, nerve terminals were stained with anti-synaptophysin antibody (A0010, DAKO) and with anti-neurofilament antibody (MAB1621, Chemicon). Secondary antibodies were from Invitrogen.

Generation of Transgenic Mice

MCK-emb—Mouse full-length embigin cDNA was amplified from reverse-transcribed denervated gastrocnemius RNA with the primers: 5′-CCATGCGCTCGCACACTGGC-3′ and 5′-GTATTCACTGATCTGCAGA-3′. The PCR amplification product was purified on a QIAquick® column (Qiagen) and subcloned into pGEM-T easy vector (Promega). The full-length mouse embigin cDNA was cut out of the pGEM-T-easy vector with EcoRI and subcloned into pBSII KS previously cut with EcoRI (Stratagene). The insert was then cut out with NotI and ClaI and subcloned into the pBSIIKS plasmid containing the MCK promoter linearized with NotI and ClaI (20).

*MCK-embigin*Δ*IC*—The truncated form of embigin lacking the intracellular domain was generated by PCR from the pGEM-T easy-embigin vector described above using the primers: 5′-CCGGAATTCATGCGCTCGCACACTGGC-3′ and 5′-GCTCTAGACTTGTGTGTGTACACTTCA-3′. The sequence was inserted in pBSII containing the MCK promoter between EcoRI and XbaI. This design eliminated 39 of 47 amino acids of the intracellular domain of wt embigin, including all potential phosphorylation sites. The eight remaining amino acids were left to ensure correct insertion into the cell membrane.

For pronuclear injections, the resulting plasmids were linearized with PacI, gel-purified with a QIAquick® Gel Extraction Kit (Qiagen), and repurified on a GeneClean Spin Column (Bio101, Qbiogene). Other mouse mutants used were: Thy-YFP mice (TgN(THY1-YFP)JRS (21)), MCK-MuSK (22), Hb9-agrin (23), and NCAM$^{-/-}$ (24).

Genotyping Transgenic Mice

Mouse toes or tails were lysed overnight at 55 °C in 500 μl of lysis buffer (50 mM KCl, 10 mM Tris-HCl, pH 8.3, 2.5 mM $MgCl_2$, 0.1 mg gelatin, 0.45% Nonidet P-40, 0.45% Tween 20) in the presence of 0.4 mg/ml proteinase K. Proteinase K was inactivated for 10 min at 95 °C. Then, the lysate was centrifuged at 14,000 rpm for 5 min at room temperature. PCR reactions on 2 μl of crude lysate were done with AmpliTaq (Roche Applied Science) in a total volume of 25 ml in the presence of 400 mM dNTPs and 400 nM each of forward and reverse primers. MCK-embigin and MCK-embDIC transgenic mice were screened for a 400-bp fragment amplified with primers 5′-CCTCCTTC-TATGTCTTCTGG-3′ and 5′-GTGGATGTTAAAGGTC-CCTC-3′ (94 °C for 2 min, 29 cycles of 94 °C for 30 s, 58 °C for 30 s, and 72 °C for 45 s, 72 °C for 7 min). MCK-musk transgenic mice were screened for a 500-bp fragment amplified with primers 5′-GAAGCAACCTTTCCTTCCTGAG-3′ and 5′-ATTT-TCCCTGAGAGCATTGTCC-3′ (94 °C for 2 min, 29 cycles of 94 °C for 20 s, 60 °C for 30 s, and 72 °C for 40 s, 72 °C for 5 min). HB9-agrin transgenic mice were screened for a 500-bp fragment amplified with primers 5′-ACCTGGATAAGCGTTTT-GTT-3′ and 5′-CTTCTGTTTTGATGCTCAGC-3′ (94 °C for 2 min, 29 cycles of 94 °C for 20 s, 54 °C for 30 s, and 72 °C for 40 s, 72 °C for 5 min). Thy1-YFP transgenic mice were screened for a 200-bp fragment amplified with primers 5′-AAGT-TCATCTGCACCACCG-3′ and 5′-TCCTTGAAGAAGATG-GTGCG-3′ (94 °C for 2 min, 34 cycles of 94 °C for 30 s, 52 °C for 30 s, and 72 °C for 30 s, 72 °C for 3 min).

Embigin Silencing

Three distinct 19-nucleotide shRNA sequences against embigin were generated using the small interference RNA selection program of the Whitehead Institute. The oligonucleotides containing the corresponding DNA sense and antisense strands were designed and inserted in the LVTHM vector, kind gift from Didier Trono, Lausanne, Switzerland. The LVTHM construct was used for both electroporation- and lentiviral-mediated gene delivery, to have a direct comparison of efficiency between the two approaches. RNA encoding sequences were (*a*) RNAi1-sense: 5′-GAAGTAGCTTTATGAACAA-3′, antisense: 5′-TTGTTCATAAAGCTACTTC-3′; (*b*) RNAi2-sense: 5′-GCGTGTACACAGCAACTAA-3′, antisense: 5-TTAGTT-GCTGTGTACACGC-3′; and (*c*) RNAi3-sense: 5′-GGCTCA-AGATTAAGCATCT-3′, antisense: 5′-AGATGCTTAATCTTGAGCC-3′.

RESULTS

Forced Expression of Agrin by Motor Neurons and of MuSK by Muscle Is Not Sufficient for NMJ Formation in Vivo—Given the ability of agrin to induce postsynaptic differentiation in the extrasynaptic membrane of electrically active muscle (25), an unfavorable condition for synapse formation due to low MuSK expression in extrasynaptic fiber regions (4), we examined whether ectopic endplates formed in soleus muscle of double mutant mice expressing transgenes for agrin in motor neurones (23) and MuSK in muscle (22), respectively, without the need to section the muscle's own nerve. Both mutants have been demonstrated to rescue their respective knockouts from lethality. 3–4 weeks after fibular nerve transplantation onto the proximal end-plate free zone of the soleus muscle in agrin/MuSK double mutants, the soleus muscles was examined visually for contractions in response to foreign nerve stimulation. No contraction was seen in six animals examined, indicating that synapses had not formed, despite agrin and MuSK transgene expression. In contrast, in six double mutant and four wild-type animals, soleus muscles did contract in response to foreign nerve stimulation, if the tibial nerve containing the soleus innervation had been cut 7 days prior to stimulation. These experiments demonstrate that synapse formation cannot be induced by overexpression alone of agrin by motor neurons and of MuSK by muscle fibers. The failure of transplanted nerves in the agrin/MuSK double mutants could not have been due to insufficient transgene expression levels, because both Hb9-agrin and MCK-MuSK muscles revealed nerve-free extrasyn-

aptic AChR clusters in adult muscle (22, 23). Therefore, ectopic synapse formation requires additional factors up-regulated by denervation, *e.g.* molecules promoting neuromuscular adhesion.

A Differential Display of mRNAs from Innervated versus Denervated Muscle Reveals Embigin as a Transmembrane IgSF Molecule Regulated by Muscle Activity—To identify genes encoding surface-expressed proteins depending on the state of innervation, we compared total RNAs isolated from innervated *versus* 4-day-denervated adult rat soleus muscles by mRNA differential display (26). Densitometric analysis of the autoradiographs revealed 255 PCR amplification products with a change in expression by at least 20%. These amplification products corresponded to 121 different genes. Out of these, expression of 40 genes was increased after denervation (supplemental Table S1) and was reduced for 81 others (supplemental Table S2). Sequencing identified a strongly up-regulated PCR product of 630 bp as a fragment of embigin (Embryo immunoglobulin) mRNA (supplemental Table S1).

Mouse embigin is a transmembrane glycoprotein with a protein component of 34 kDa. Cleavage of a 24-amino acid signal sequence generates the membrane-bound form consisting of two extracellular Ig domains, a transmembrane domain (29 amino acids), and a short (47 amino acids) cytoplasmic domain. It belongs to a small subgroup of Ig molecules characterized by two Ig domains and comprising, in addition to embigin, neuroplastin and basigin (EMMPRIN/CD147). Basigin is the best investigated member of this family with multiple, but poorly defined functions in reproduction, neural function, inflammation, and tumor invasion (27). The sequence homology of basigin with embigin at the amino acids level is only ~28% in the mouse, and is conspicuously concentrated in their transmembrane regions where all members of the family share a glutamic acid residue, suggesting that they associate with other transmembrane molecules to express at least some of their functions. On the other hand, embigin lacks a cluster of positively charged residues in the juxtamembrane cytoplasmic region of basigin that were recently found to be essential for normal NMJ formation and function in *Drosophila* (28). Furthermore, unlike basigin, embigin does not mediate cell aggregation by homophilic interactions (29),[3] suggesting different modes of function for the two. Given its preferential expression in the endoderm during early postimplantation embryogenesis, the major role of embigin is thought to be in early embryonic development (17, 30).

Up-regulation of embigin mRNA in muscle by denervation was confirmed by Northern blot analysis and qRT-PCR. Northern blots of mRNA from denervated mouse gastrocnemius muscle revealed strong up-regulation of two transcripts of 1.5 and 2.1 kb, generated by an alternative polyadenylation site in the 3′-untranslated region (Fig. 1*B*). The intensity of the two bands increased progressively in the post-denervation period until day 10. The temporal expression pattern of embigin mRNA upon denervation was further analyzed by quantitative PCR, in both rat soleus and mouse gastrocnemius muscles. In

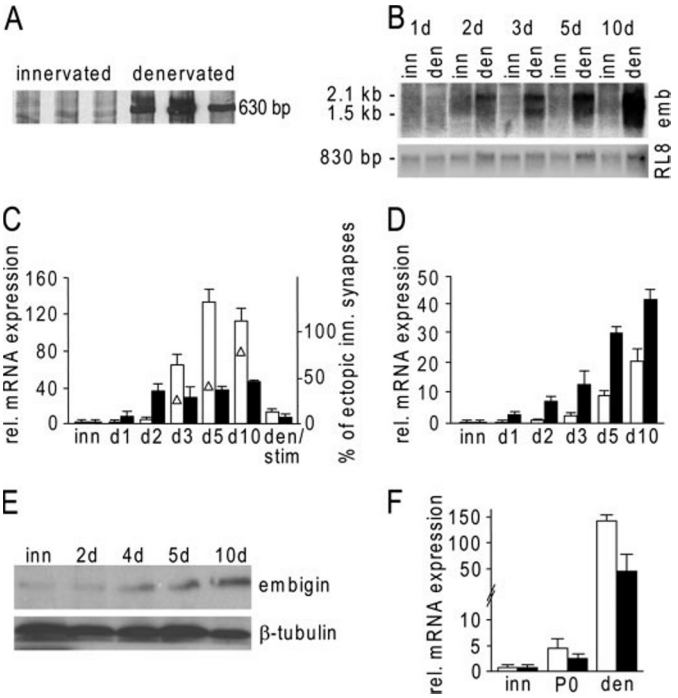

FIGURE 1. **Regulation of embigin expression in adult rodent muscle by electrical muscle activity.** *A*, autoradiography of the initial mRNA differential display experiment. Three different samples of either innervated or denervated rat soleus muscles were used for PCR amplifications and analyzed on polyacrylamide gels. The differentially regulated PCR amplification product of 630 bp corresponds to embigin mRNA. *B*, denervation-induced transcription of *embigin* analyzed by Northern blot. Expression of the ribosomal protein L8 (*RL8*) was assessed as internal standard. *C* and *D*, transcript levels of embigin (*white columns*) and AChRd (*black columns*) were measured in rat (*C*) and in mouse (*D*) soleus muscles by quantitative RT-PCR on innervated (*inn*), denervated (*d*), and denervated/stimulated (*den/stim*) muscles at various time points after denervation. Expression levels were normalized to the expression of RL8. Innervated samples were arbitrarily set to 1, and -fold inductions ± S.E. are shown ($n = 3–5$). *Open triangles* indicate the percentage of ectopically innervated surface muscle fibers as a function of time after cutting the soleus nerve (data from Ref. 32). *E*, time course of embigin protein expression by Western blot following denervation in mouse leg muscle. *Numbers* give days after denervation. β-Tubulin was used as loading control. *F*, embigin mRNA relative to RL8 mRNA expression levels in neonatal (P0) compared with innervated and denervated adult rat (*white columns*) and mouse (*black columns*) leg muscles, analyzed by quantitative RT-PCR ($n = 4$).

the rat, embigin mRNA expression was significantly increased 3 days after denervation to reach a maximum, ~130-fold increase after 5 days (Fig. 1*C*). Electrical stimulation of denervated soleus muscle via implanted electrodes, beginning at 5 days postdenervation, reduced embigin mRNA levels to control levels by day 10, demonstrating strong regulation by electrical muscle activity (Fig. 1*C*). In the mouse, the maximum expression occurred at day 10, the last day examined (Fig. 1*D*), when an increase in mRNA level by ~20-fold was measured. Western blot analysis on mouse (Fig. 1*E*) muscles revealed up-regulation, although more moderate, also at the protein level. Interestingly, the increase in embigin mRNA expression following denervation parallels the onset of extrasynaptic expression of genes involved in synapse formation (AChR δ-subunit, musk (4, 31)), as well as the formation of ectopic synapses by transplanted foreign nerves after the soleus nerve is sectioned (32) (Fig. 1*C*), consistent with the idea that it may be related to ectopic synapse formation.

[3] S. Carnejac, unpublished observation.

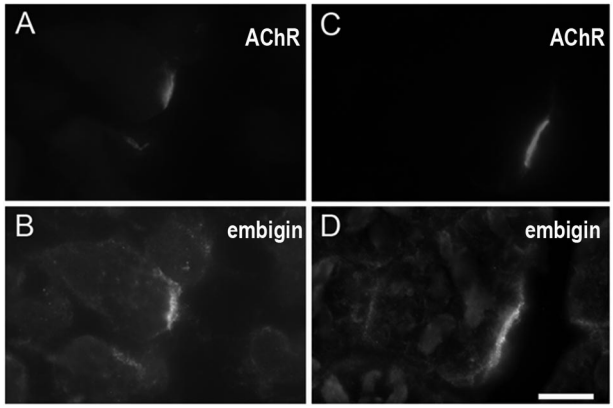

FIGURE 2. **Embigin is localized to the neuromuscular junction in neonatal (P0; *A* and *B*) and in adult (P126; *C* and *D*) soleus muscles.** Embigin immunoreactivity (*B* and *D*) and synaptic AChR clusters resolved by α-Bgt staining (*A* and *C*) are shown in cross-sections of rat leg muscle. Incubation in primary antibody in the presence of immunizing peptide abolished synapse-specific staining (not shown). *Bar*: 10 μm.

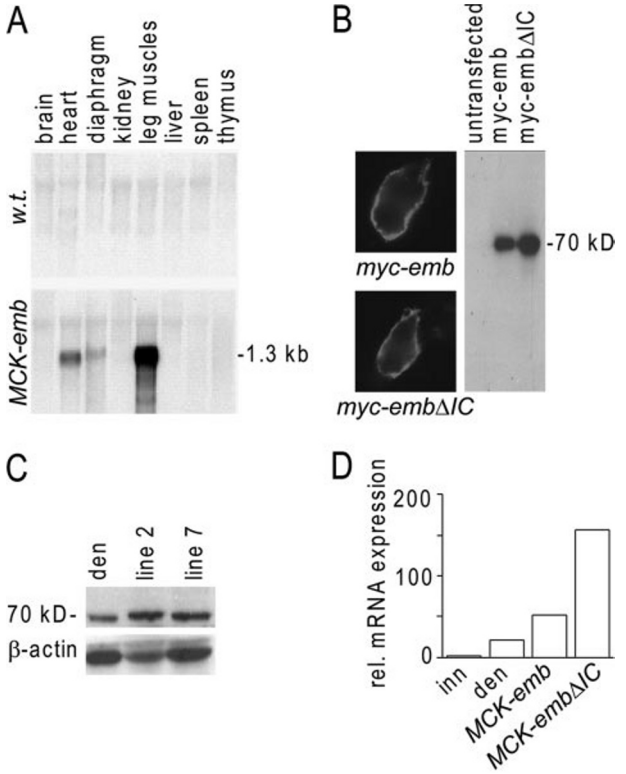

FIGURE 3. **Embigin expression in MCK-emb transgenic mouse lines.** *A*, Northern blot analysis in various organs of adult wild-type and MCK-emb mice shows strong embigin mRNA expression in the leg muscles of transgenic animals (*line 3*). *B*, protein products of transgenes used for setting up transgenic lines are directed to the cell membranes of HEK293 cells. The full-length and truncated embigin expression constructs tagged in c-Myc in their N termini were transfected into HEK293 cells. c-Myc-immunoreactivities in non-permeabilized HEK293 cells are shown. Western blot analysis confirms the specificity of the antibody for the c-Myc-tagged forms of embigin. The difference in calculated molecular weight between full-length (330 amino acids) and truncated embigin (290 amino acids) is not resolved on this blot because the deleted intracellular domain (calculated to be 4.5 kDa) is only 5% of the molecular mass of the glycolyated full-length protein with an molecular mass of 70 kDa (hence also called gp70), taking also the molecular weight of the Myc tags into account. *C*, Western blot analysis of embigin in mouse soleus muscles, using a rabbit polyclonal antibody. Two transgenic mouse lines (*2* and *7*) were tested, and expression levels were compared with a denervated wt sample. β-Actin was used as loading control. *D*, relative mRNA expression of embigin in denervated wild types, MCK-emb (*line 2*) and MCK-embDIC transgenic mice, measured by qRT-PCR. The value in innervated samples was set to 1.

Next, we examined the expression of embigin in developing muscle. Unlike *AChR* subunit genes, which are expressed at substantially higher levels in neonatal than in adult muscle (33), embigin mRNA in leg muscle at P0 was only moderately (5-fold) higher than in the adult (Fig. 1*F*). Nevertheless, immunocytochemistry showed that it was localized to the endplates at this stage of development and remained concentrated at the synapse throughout adult life (Fig. 2).

Embigin Overexpression Induces Ultraterminal Sprouts Followed by AChR Clusters—To test for a physiological function of embigin at the NMJ *in vivo*, five lines of transgenic mice overexpressing embigin under the control of the muscle creatine kinase (MCK) promoter were generated (for characterization, see Fig. 3), and effects on NMJ morphology were observed. In soleus muscles of two lines embigin transgenic protein expression levels were comparable with endogenous protein levels in wild-type muscles after denervation (Fig. 3*C*). Embigin overexpression affected the morphology of the NMJ. To visualize motor axons and their terminal arborizations, *embigin* mutants were crossed with a transgenic line expressing yellow fluorescent protein in the cell membrane of neurones, or nerve terminals were visualized by immunocytochemistry. AChR receptors were stained with α-bungarotoxin-Alexa594. Many nerve terminals in adult muscles of the three transgenic lines showing comparable levels of embigin transgene mRNA (lines 2, 5, and 7; 12–16 weeks old) developed terminal sprouts. The sprouts were thin terminal extensions growing beyond the region of AChR clusters and often ending in wider circular shapes (Fig. 4*B*). The latter were not seen in wt muscles. Some, but not all of the circular extensions were colocalized with AChR clusters (Fig. 4*A*), suggesting that the sprouts induced the clusters rather than vice versa. In one line (no. 2) the occurrence of terminal sprouting was compared quantitatively with that in wild-type littermates, taking only sprouts into account that were not apposed by AChR clusters. In control animals sprouts were seen in 5.4 $\pm$ 0.9% of all endplates (S.E.; $n = 3$), in the MCK-emb mutants they occurred in 22.4 $\pm$ 2.3% (S.E.; $n = 5$) (Fig. 4*C*) of endplates examined. Enhanced sprouting in the *embigin* mutants was not restricted to soleus muscles but was also seen in two diaphragm and in one transgenic tibialis anterior muscles where it was increased 3.2- and 5-fold, respectively, compared with controls (100 synapses examined in each muscle). Importantly, the 22% occurrence of sprouts was derived from those endplates only where sprouts did not induce additional postsynaptic AChR clusters (as *e.g.* in Fig. 4*B*). Given that many do induce subclusters the fraction of endplates exhibiting sprouts as shown in Fig. 4*C* is an underestimate only of the sprout-inducing action of embigin overexpression in innervated muscle. These data combined indicate, therefore, that embigin expression levels in innervated muscles similar to those seen in wild types after denervation cause the formation of ultraterminal sprouts.

The effect of embigin overexpression to induce terminal sprouts at innervated endplates was dependent on the presence of its intracellular domain. Specifically, in two mouse lines

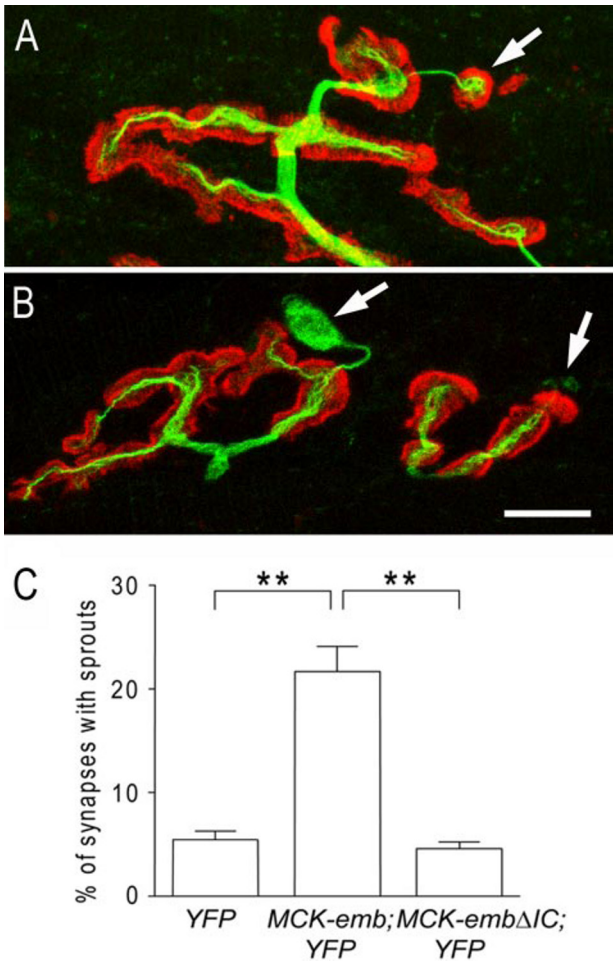

FIGURE 4. **Overexpression of embigin transgene in innervated soleus muscle induces nerve terminal sprouting that is dependent on the presence of embigin intracellular domain.** *A* and *B*, in embigin full-length mutant animals, motoneurons (*green*) grow beyond the AChR clusters (*red*) stained with α-bungarotoxin-Alexa594. Sprouts are marked by *arrows*. The presence of small AChR clusters can be observed at the end of some sprouts (*A*, *arrow*). *C*, in comparison to wt littermates (*left bar*), the percentage of synapses exhibiting terminal sprouts is significantly increased in mice overexpressing full-length (*center bar*) but not truncated embigin (*right bar*). Only synapses with sprouts not apposed to AChR cluster such as in *B* were counted. Results are expressed as mean ± S.E. (n = 3–5; 21–78 analyzed synapses/animal; **, $p < 0.01$; *line 2*). *Bar*: 10 μm.

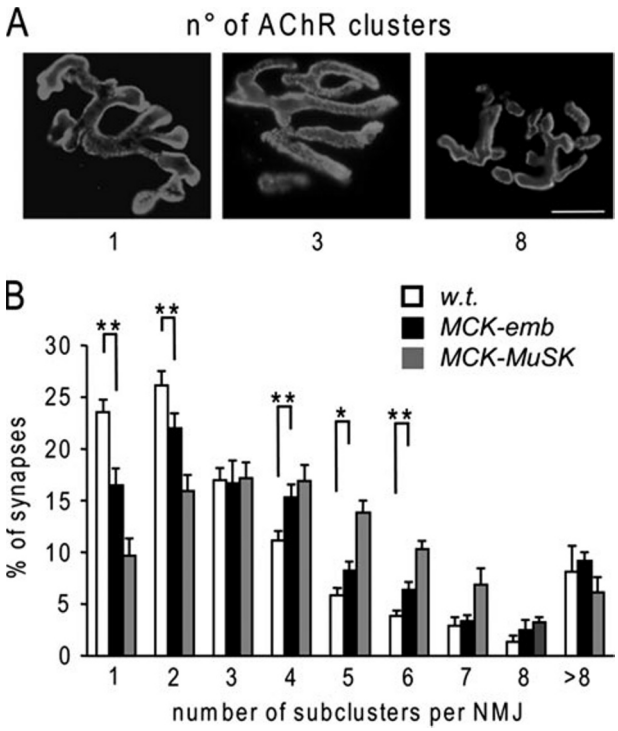

FIGURE 5. **Number of AChR clusters per synapse is increased in MCK-embigin soleus muscles.** *A*, examples of endplates composed of different numbers of AChR clusters (given below the *micrographs*). *B*, in mutant mice (n = 10), the number of clusters per endplate was significantly increased in comparison to wt littermates (n = 9). An increase was observed also in MCK-MuSK mice (n = 6). Results are represented as mean ± S.E. (77–167 synapses analyzed/animal; **, $p < 0.01$; *, $p < 0.05$). *Bar*: 10 μm.

overexpressing similar or higher levels of mRNA encoding a truncated embigin (MCK-embΔIC; lacking 39 of 47 amino acids of the intracellular domain of wt embigin) than the MCK-emb lines, the percentage of endplates exhibiting terminal sprouts was similar as in wt muscles (Fig. 4*C*). Control experiments showed that the embΔIC transgene mRNA was expressed at higher level than that of the full-length embigin transgene in the MCK-emb lines, and that both transgene products were expressed at comparable levels in cell membranes (Fig. 3, *B* and *D*). Therefore, the absence of sprouts in the MCK-embΔIC mice was not due to differences in expression levels, or of defective trafficking and membrane insertion of the embΔIC transgene product.

If embigin-induced terminal sprouting can induce additional AChR clusters as speculated above, the number of small separate AChR clusters at an endplate should be increased. Consistent with this notion, endplates in transgenic muscles revealed a higher number of AChR "subclusters" per endplate than wt soleus (Fig. 5). Interestingly, a similar but more pronounced effect was seen in the mice overexpressing *musk* (MCK-musk, Fig. 5), consistent with the idea that the induction of additional subclusters is promoted in two ways: (*a*) by additional sprouts stabilized by embigin-induced, neuromuscular adhesion that in turn results in a strong deposit of agrin on a fiber with normal level of surface MuSK, or (*b*) by sprouts of low stability resulting in a weak deposit of agrin on a fiber with high level of surface MuSK.

At early stages of development, vertebrate muscle fibers are innervated by several motor neurons over a protracted period of time. During the first two postnatal weeks motor axons compete for the sole innervation of muscle fibers in a process known as synapse elimination (34). The action of stabilizing/destabilizing factors cleaving adhesive links between nerve terminals, the basal lamina, and muscle fibers and thus promoting synapse loss has been suggested to mediate this elimination. Because embigin is expressed at synapses at P0 and delays retraction of terminal sprouts in adults (see below) we examined whether synapse elimination was delayed in the MCK-emb mice by comparing the percentage of poly-innervated endplate sites in transgenic and wild-type animals at postnatal days 2, 4, 8, and 12. No difference in the time course of the synapse elimination could be resolved (data not shown).

Retraction of Terminal Sprouts upon Re-innervation of Denervated Endplates Is Delayed by Embigin Overexpression—Sprouting of nerve terminals is a normal consequence of neu-

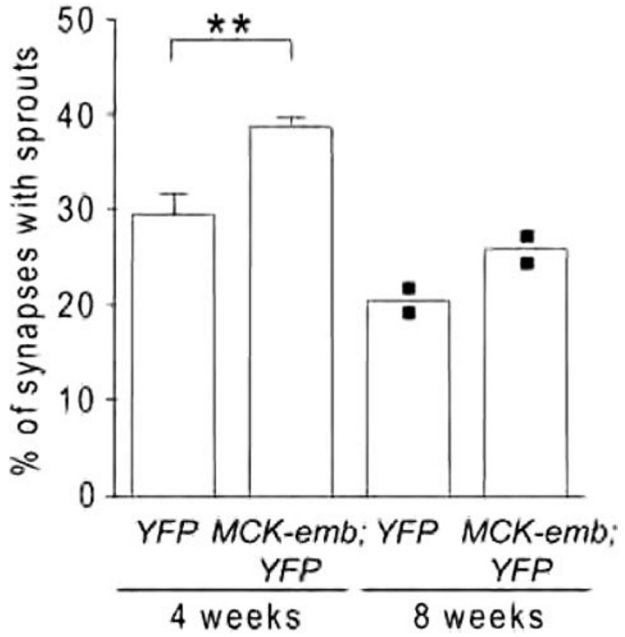

FIGURE 6. **The retraction of terminal sprouts following re-innervation is delayed in MCK-Emb mice (line 2).** When endplates were re-innervated following nerve crush, sprouts grew beyond synaptic AChR clusters marked by staining with α-bungarotoxin-Alexa594 and then retracted (for illustration, see Fig. 7*C*). Retraction was delayed in MCK-emb mice. *Bars* show percentage of synapses 4 and 8 weeks after nerve crush. Results are expressed as mean ± S.E. (4 weeks: $n = 6–7$; 30 synapses analyzed/animal; **, $p < 0.01$; 8 weeks: mean from $n = 2$ animals is shown).

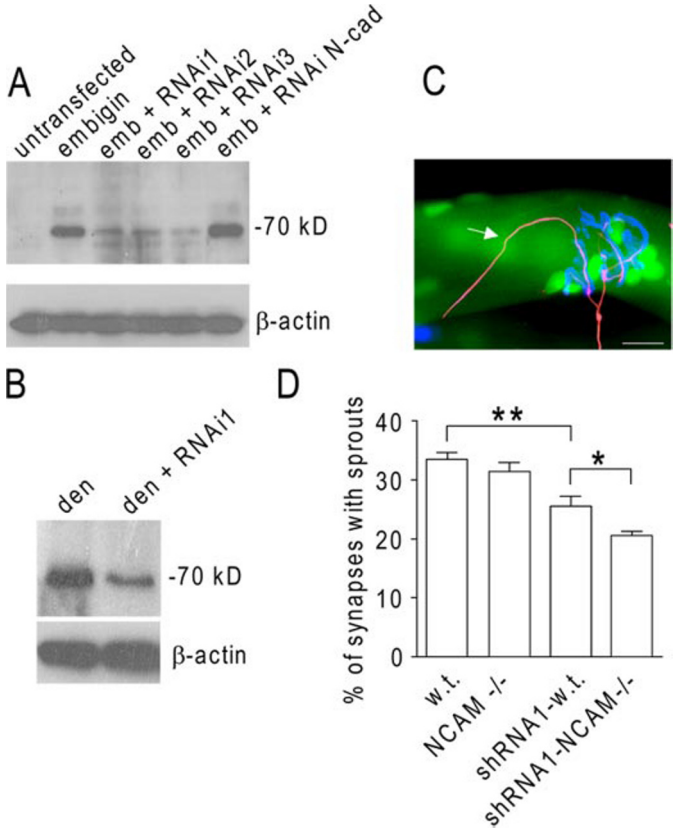

FIGURE 7. **Inhibition of embigin expression by RNAi accelerates retraction of terminal sprouts at endplates re-innervated after nerve crush.** *A*, test of efficiency to knockdown embigin expression by three different constructs encoding nuclear localisation signal-GFP and shRNA directed against embigin mRNA. HEK 293 cells were transfected with cDNA constructs encoding embigin alone or combined with one of three different constructs expressing shRNA (RNAi1, RNAi2, and RNAi3) designed to knock down embigin expression, and expression levels of embigin protein were analyzed by Western blot. Note that the intensity of the embigin band (70 kb) was strongly reduced after co-transfection with all three knockdown constructs. No reduction was seen after cotransfection of the same vector expressing shRNA against (unrelated) N-cadherin (*RNAi N-cad*). *B*, electroporation of the RNAi1 construct into mouse soleus muscles strongly reduces up-regulation or embigin protein by denervation. *Den*: denervated samples. β-Actin was used as loading control. *C*, example of terminal sprout (*arrowhead*) at re-innervated endplate 4 weeks after nerve crush. Axons were stained for neurofilaments (*red*) and synaptic AChRs with α-bungarotoxin-Alexa647 (*blue*), respectively. In electroporated muscles sprouts were counted only in fibers that had been transfected with knockdown constructs. They were marked by their expression of GFP (*green*). *D*, retraction of terminal sprouts formed at re-innervated endplates is accelerated by knockdown of embigin expression. The percentage of endplates exhibiting sprouts in the injected wild-type muscles (*shRNA1-WT*) was significantly lower than in the contralateral muscles (*WT*), which were taken as controls ($n = 8$; total of 163–191 synapses analyzed; **, $p < 0.01$). A further reduction in the number of endplates exhibiting sprouts was measured in transfected fibers of NCAM-deficient animals (shRNA1-NCAM$^{-/-}$) in comparison to shRNA1-WT fibers ($n = 8$, 150–196 synapses; *, $p < 0.05$). No significant difference in the sprouting response between WT and NCAM$^{-/-}$ samples was resolved. Results are expressed as mean ± S.E. *Bar*: 20 μm.

romuscular inactivity (35, 36). Terminals also grow beyond endplate AChR clusters when they re-innervate them following denervation. Once the transmission is restored, sprouts tend to retract (37). To see whether embigin expression levels affected retraction of terminal sprouts formed by axons re-innervating denervated endplate sites, we denervated wild-type and embigin overexpressing soleus muscles by crushing the sciatic nerves at identical levels of the thigh and counted the fraction of endplates with sprouts 4 weeks later. Consistent with a positive effect of embigin on terminal sprouting, the percentage of endplates with sprouts at this time was higher in MCK-emb mutants (38.6 ± 1.1%, S.E., $n = 180$ synapses in 6 animals) than in wild-type animals (29.4 ± 2.2%; S.E., $n = 210$ synapses in 7 animals) (Fig. 6). A similar difference was found in muscles examined 8 weeks after the nerve crush. By this time the level of endogenous embigin mRNA expression was down-regulated to normal (data not shown), indicating that the delay in sprout retraction in the mutant mice was caused by the *embigin* transgene expression.

If so, lowering expression levels should accelerate it. We tested this prediction by monitoring the number of terminal sprouts remaining 4 weeks after nerve crush in denervated muscle in which endogenous embigin expression had been knocked down by RNA interference (RNAi). In a first step, three constructs expressing different sequences of small hairpin RNA (shRNA) were positively tested by Western blotting for their ability to knock down embigin protein in HEK293 cells induced to express embigin by co-transfection of an expression construct (Fig. 7*A*). An unrelated shRNA construct used for knockdown of N-cadherin (38) served as a control for specificity (Fig. 7*A*). Knockdown of embigin was also seen when these shRNA constructs were electroporated into denervated soleus muscle (Fig. 7*B*), but less pronounced than in HEK293 cells. At least in part, this difference can be ascribed to the fact that at most 50% of all fibers in a muscle are electroporated by the method used (see below). To examine the effect of embigin knockdown on sprout retraction, the sciatic nerve of wild-type mice was crushed bilaterally, and the construct encoding the

shRNA was electroporated into the soleus muscle only on one side, together with a nuclear localisation-GFP-expressing construct to mark transfected fibers. Four weeks later the percentage of synapses displaying sprouts was 25.4 ± 1.9% (Fig. 7*D*; S.E., $n = 191$ synapses in 8 animals) in the GFP-positive fibers transfected with shRNA (Fig. 7*C*), and it was 33.5 ± 1.0% (S.E., $n = 163$ synapses in 8 animals) in control fibers not treated with shRNA. In innervated muscles electroporated with an expression construct for GFP alone the percentage of endplates with terminal sprouts (5.4 ± 0.7%, S.E., 108 synapses in 4 animals) was similar as in normal muscle (5.4 ± 0.9%, S.E., see Fig. 4), indicating that electroporation *per se* did not affect sprouting. Thus, knockdown of endogenous embigin significantly accelerated sprout retraction upon re-innervation. These experiments combined support the notion that the level of ultraterminal sprouting is positively correlated with the level of embigin expression.

Sprout Retraction by Embigin Knockdown Is Potentiated in the Absence of NCAMs—In adult muscle expression of NCAMs is regulated in parallel with embigin: it is localized to the neuromuscular junction, up-regulated upon denervation, and lost again upon re-innervation (39, 40). Because both embigin and NCAM (10) promote terminal sprouting when overexpressed, we next examined the sprout numbers upon re-innervation in NCAM mutant mice in which endogenous embigin was down-regulated by RNAi. Whereas, in accordance with Ref. 15, the lack of NCAM alone did not significantly affect retraction of sprouts upon re-innervation compared with wild types (Fig. 7*D*), the knockdown of embigin in NCAM$^{-/-}$ mutants significantly accelerated sprout retraction compared with that observed in either control NCAM$^{-/-}$ muscles or in wt muscles upon embigin knockdown (Fig. 7*D*; 20.5 ± 2.4% of synapses with sprouts; $p < 0.05$). Thus, with regard to sprout retraction upon re-innervation the effect of embigin knockdown was stronger that that of NCAM deletion.

Embigin Overexpression Does Not Affect the Extensions of Terminal Schwann Cells—After partial muscle denervation terminal Schwann cells extend processes both in those endplates that had been denervated and those remaining innervated (41–43). These Schwann cell extensions guide terminal sprouts growing from innervated endplates to re-innervate adjacent denervated endplate sites (44). To test for a potential involvement of Schwann cells in embigin-induced ultraterminal sprouting, their morphology was compared in mutant and wt animals by immunohistochemical staining with an antibody against the small calcium-binding protein S100. In most endplates both in mutant and wt soleus muscle, Schwann cells were coextensive with motor nerve terminals. Small ultraterminal extensions were seen in 23.5 ± 1.7% of endplates (S.E.; $n = 145$ in 4 animals) in MCK-emb and in 23.1 ± 1.2% of endplates (S.E.; $n = 143$ in 4 animals) in soleus muscle of wild-type littermates (Fig. 7), in accordance with a previous report (44). Thus, we were unable to resolve any evidence of an involvement of Schwann cells in the induction of Embigin-induced sprouting of motor nerve terminals.

DISCUSSION

We have found the small transmembrane molecule embigin to be expressed in mammalian skeletal muscle with a spatiotemporal pattern and function that are consistent with its involvement in NMJ formation and during muscle re-innervation following nerve lesions. Specifically, embigin is expressed in developing muscle (P0), is down-regulated in the adult, is concentrated at the NMJ from P0 throughout postnatal life, and is strongly up-regulated upon denervation as a consequence of the lack of impulse activity. Following denervation, embigin expression is increased with a time course that parallels the increase of *AChR*δ-subunit expression and the formation of ectopic synapses by transplanted foreign nerves (32). Furthermore, overexpression in adult innervated muscle elicits the formation of ultraterminal sprouts inducing additional AChR clusters. Embigin expression levels also affect the time course of sprout retraction after endplates are re-innervated upon nerve crush: Overexpression delays and knockdown by RNAi accelerates the retraction of ultraterminal sprouts. Sprout retraction is further accelerated when embigin expression is knocked down in NCAM-deficient muscle. Finally, ultraterminal sprout induction by embigin is dependent on the presence on its intracellular domain.

In adult mammalian muscle embigin or basigin are required for expression and activity of monocarboxylate transporters MCT1–MCT4 in the muscle fiber membrane (19). However, upon denervation the strong up-regulation of embigin observed here contrasts with the concomitant decline of MCT mRNA levels.[4] Remarkably, denervation in muscle is the strongest stimulus for embigin expression observed so far.

The effects of embigin in muscle to induce terminal sprouts and to delay sprout retraction upon re-innervation synergistically with NCAM are consistent with the idea that embigin promotes the adhesion of motor neurites to the muscle surface. Specifically, the sprouts seen at 5% of NMJs in wild-type muscle may reflect the result of spontaneous outgrowth and regression of terminal extensions, as has been previously observed at the mouse NMJ (45). Their increased adhesion to the muscle fiber surface by elevated embigin would stabilize sprouts that in its absence might regress, thus increasing their occurrence in the transgenic muscle. Similarly, increased stability of the sprouts can explain the induction of new AChR subclusters (Fig. 5), because stable sprouts can stably deposit agrin in the basal lamina of the muscle fiber, a condition for recombinant agrin to induce ectopic AChR clusters in non-synaptic muscle membrane (5). This would result in increased number of AChR clusters at an endplate. With a similar result, overexpression of MuSK makes the fibers more sensitive to deposits of low agrin concentration that in wt muscle with normal low perisynaptic MuSK levels may remain below threshold for the induction of additional AChR clusters.

Based on current concepts of neuromuscular interactions embigin overexpressed in muscle could promote sprouting of nerve terminals in the following ways: by signaling through Schwann cells and/or by increasing neurite adhesion to the

[4] P. Escher and H. R. Brenner, unpublished observation.

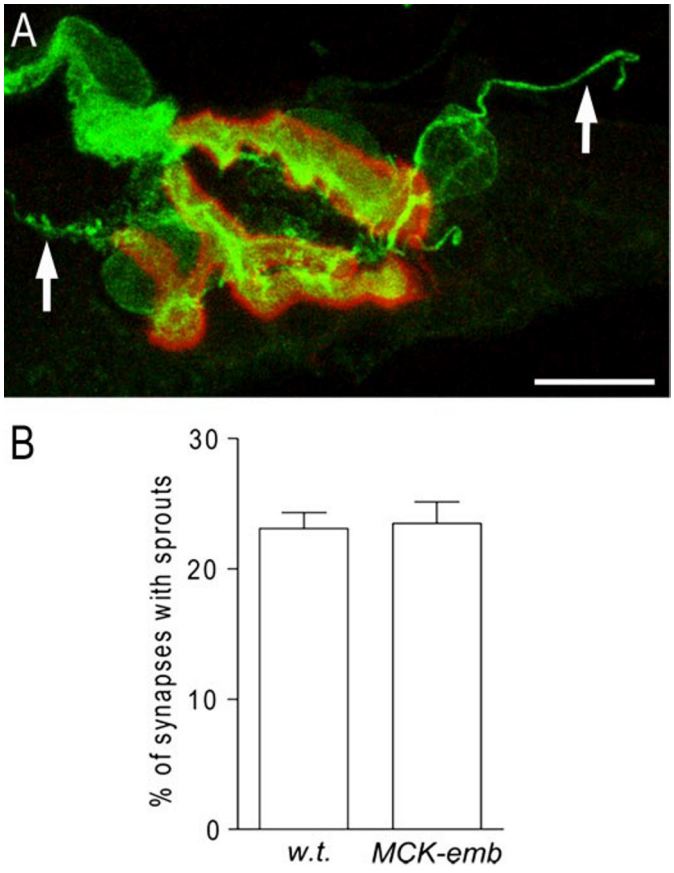

FIGURE 8. **Schwann cell processes extending beyond the synaptic AChR cluster are present in equal measure in the soleus muscle of MCK-emb mice and wt littermates.** *A*, Schwann cell processes marked by arrows. *Bar*, 10 μm. *B*, *bars* show percentage of synapses with sprouts (mean $\pm$ S.E.; $n = 4$; 143–145 synapses analyzed).

muscle surface; in turn, such adhesion could be mediated via direct or indirect, *e.g.* NCAM-mediated interaction of embigin in the muscle surface with molecules in the neurite surface. Alternatively embigin may interact with NCAM on the membrane surface to inhibit ectodomain shedding by metalloproteases. Regulated metalloprotease-induced ectodomain shedding of NCAM has been shown to down-regulate neurite branching and outgrowth (46).

Evidence against an action through Schwann cells is that the number of endplates with Schwann cell extensions in innervated wt muscle is similar to that in innervated MCK-emb muscle (Fig. 8). On the other hand the fraction of NMJs with Schwann cell extensions both in innervated wt and in MCK-emb muscles (23%, Fig. 8) equals the fraction of NMJs in MCK-emb muscles forming sprouts (22%, Fig. 4), consistent with the idea that Schwann cell extensions may be permissive for embigin-induced terminal sprouting.

Likewise, embigin in muscle is unlikely to promote sprouting via homophilic interactions with embigin in the nerve cell membrane, because expression of embigin in HEK cells does not increase their adhesiveness to one another[5] and because its extracellular domain appears too short to span the synaptic cleft. Therefore, direct neuromuscular interactions involving embigin would imply binding on the neural surface to a molecule with a longer extracellular domain. Binding would be modulated via inside-out signaling, because the effect of embigin on terminal sprouting depends on its intracellular domain (Fig. 4).

Finally, embigin may induce terminal spouting by modulating adhesion mediated by other CAMs, such as NCAM. In muscle NCAM is expressed with a spatiotemporal pattern similar to that found here for embigin (47), and when overexpressed in innervated muscle it induces terminal sprouts (10) by binding to its homolog on the motor neuron (9). Sprout retraction upon re-innervation is delayed when embigin is overexpressed (Fig. 6). Conversely, retraction is accelerated when embigin expression is knocked down by RNAi; it is accelerated further by combined embigin knockdown and lack of NCAM (see Fig. 7), although sprouts in wild-type muscle take weeks to retract (Fig. 6), *i.e.* much longer than both molecules take for down-regulation to normal levels after NMJs are re-innervated (Figs. 1 and 6). This indicates that sprout retraction upon re-innervation is not tightly linked to the levels of embigin and NCAM, but may depend on other (adhesive) interactions. Given that the lack of NCAM alone did not affect sprout retraction, and that the major NCAM isoform expressed in response to denervation lacks an intracellular domain (but is glycosylphosphatidylinisotol-linked NCAM120 (46)), the potentiation of sprout retraction by combined embigin-knockdown and NCAM deletion suggests that embigin may directly or indirectly modulate NCAM function through both its intra- and extracellular domains. Indirect modulation seems more likely, because co-immunoprecipitation experiments did not reveal physical interaction between NCAM120 and embigin when coexpressed in HEK293 cells or in C2C12 muscle cells.[6]

In summary, independently of the precise mode of the actions of embigin, its expression patterns during development and upon denervation paralleling those of NMJ formation and of the susceptibility of the muscle to innervation, its ability to promote terminal sprouts inducing AChR clusters, and its functional synergism with NCAM, indicate that it joins the family of CAMs involved in neuromuscular synapse formation and plasticity.

REFERENCES

1. Kim, N., and Burden, S. J. (2008) *Nat. Neurosci.* **11,** 19–27
2. Bezakova, G., and Ruegg, M. A. (2003) *Nat. Rev. Mol. Cell. Biol.* **4,** 295–308
3. Lømo, T. (2003) *J. Neurocytol.* **32,** 835–848
4. Bowen, D. C., Park, J. S., Bodine, S., Stark, J. L., Valenzuela, D. M., Stitt, T. N., Yancopoulos, G. D., Lindsay, R. M., Glass, D. J., and DiStefano, P. S. (1998) *Dev. Biol.* **199,** 309–319
5. Meier, T., Marangi, P. A., Moll, J., Hauser, D. M., Brenner, H. R., and Ruegg, M. A. (1998) *Eur. J. Neurosci.* **10,** 3141–3152
6. Storms, S. D., Anvekar, V. M., Adams, L. D., and Murray, B. A. (1996) *Exp. Cell Res.* **223,** 385–394
7. Burg, M. A., Halfter, W., and Cole, G. J. (1995) *J. Neurosci. Res.* **41,** 49–64
8. Cotman, S. L., Halfter, W., and Cole, G. J. (1999) *Exp. Cell Res.* **249,** 54–64
9. Walsh, F. S., and Doherty, P. (1997) *Annu. Rev. Cell Dev. Biol.* **13,** 425–456
10. Walsh, F. S., Hobbs, C., Wells, D. J., Slater, C. R., and Fazeli, S. (2000) *Mol. Cell Neurosci.* **15,** 244–261
11. Niethammer, P., Delling, M., Sytnyk, V., Dityatev, A., Fukami, K., and Schachner, M. (2002) *J. Cell Biol.* **157,** 521–532

[5] S. Carnejac and H. R. Brenner, unpublished observation.

[6] S. Hashemolhosseini, personal communication.

12. Sanes, J. R., Schachner, M., and Covault, J. (1986) *J. Cell Biol.* **102,** 420–431
13. Gatchalian, C. L., Schachner, M., and Sanes, J. R. (1989) *J. Cell Biol.* **108,** 1873–1890
14. Wehrle-Haller, B., and Chiquet, M. (1993) *J. Cell Sci.* **106,** 597–610
15. Moscoso, L. M., Cremer, H., and Sanes, J. R. (1998) *J. Neurosci.* **18,** 1465–1477
16. Radice, G. L., Rayburn, H., Matsunami, H., Knudsen, K. A., Takeichi, M., and Hynes, R. O. (1997) *Dev. Biol.* **181,** 64–78
17. Huang, R. P., Ozawa, M., Kadomatsu, K., and Muramatsu, T. (1990) *Differentiation.* **45,** 76–83
18. Windisch, A., Gundersen, K., Szabolcs, M. J., Gruber, H., and Lømo, T. (1998) *J. Physiol.* **510,** 623–632
19. Wilson, M. C, Meredith, D., Fox, J. E., Manoharan, C., Davies, A. J., and Halestrap, A. P. (2005) *J. Biol. Chem.* **280,** 27213–27221
20. Moll, J., Barzaghi, P., Lin, S., Bezakova, G., Lochmüller, H., Engvall, E., Müller, U., and Ruegg, M. A. (2001) *Nature* **413,** 302–307
21. Feng, G., Mellor, R. H., Bernstein, M., Keller-Peck, C., Nguyen, Q. T., Wallace, M., Nerbonne, J. M., Lichtman, J. W., and Sanes, J. R. (2000) *Neuron* **28,** 41–51
22. Herbst, R., Avetisova, E., and Burden, S. J. (2002) *Development* **129,** 5449–5460
23. Ksiazek, I., Burkhardt, C., Lin, S., Seddik, R., Maj, M., Bezakova, G., Jucker, M., Arber, S., Caroni, P., Sanes, J. R., Bettler, B., and Ruegg, M. A. (2007) *J. Neurosci.* **27,** 7183–7195
24. Cremer, H., Lange, R., Christoph, A., Plomann, M., Vopper, G., Roes, J., Brown, R., Baldwin, S., Kraemer, P., Scheff, S., Barthels, D., Rajewsky, K., and Wille, W. (1994) *Nature.* **367,** 455–459
25. Jones, G., Meier, T., Lichtsteiner, M., Witzemann, V., Sakmann, B., and Brenner, H. R. (1997) *Proc. Natl. Acad. Sci. U. S. A.* **94,** 2654–2659
26. Liang, P., and Pardee, A. B. (1992) *Science.* **257,** 967–971
27. Hayworth, C. R., Moody, S. E., Chodosh, L. A., Krieg, P., Rimer, M., and Thompson, W. J. (2006) *J. Neurosci.* **26,** 6873–6884
28. Besse, F., Mertel, S., Kittel, R. J., Wichmann, C., Rasse, T. M., Sigrist, S. J., and Ephrussi, A. (2007) *J. Cell Biol.* **177,** 843–855
29. Huang, R. P, Ozawa, M., Kadomatsu, K., and Muramatsu, T. (1993) *Dev. Biol.* **155,** 307–314
30. Fan, Q. W., Kadomatsu, K., Uchimura, K., and Muramatsu, T. (1998) *Dev. Growth Differ.* **40,** 277–286
31. Witzemann, V., Brenner, H. R., and Sakmann, B. (1991) *J. Cell Biol.* **114,** 125–141
32. Lømo, T., and Slater, C. R. (1978) *J. Physiol.* **275,** 391–402
33. Witzemann, V., Barg, B., Criado, M., Stein, E., and Sakmann, B. (1989) *FEBS Lett.* **242,** 419–424
34. Sanes, J. R., and Lichtman, J. W. (1999) *Annu. Rev. Neurosci.* **22,** 389–442
35. Brown, M. C., and Ironton, R. (1977) *Nature* **265,** 459–461
36. Brown, M. C., and Holland, R. L. (1979) *Nature* **282,** 724–726
37. Brown, M. C., Holland, R. L., and Hopkins, W. G. (1981) *Annu. Rev. Neurosci.* **4,** 17–42
38. Maeda, M., Johnson, K. R., and Wheelock, M. J. (2005) *J. Cell Sci.* **118,** 873–887
39. Moore, S. E., and Walsh, F. S. (1985) *EMBO J.* **4,** 623–630
40. Covault, J., and Sanes, J. R. (1986) *J. Cell Biol.* **102,** 716–730
41. Son, Y. J., and Thompson, W. J. (1995) *Neuron* **14,** 125–132
42. Son, Y. J., and Thompson, W. J. (1995) *Neuron* **14,** 133–141
43. O'Malley, J. P., Waran, M. T., and Balice-Gordon, R. J. (1999) *J. Neurobiol.* **38,** 270–286
44. Muramatsu, T., and Miyauchi, T. (2003) *Histol. Histopathol.* **18,** 981–987
45. Wigston, D. J. (1989) *J. Neurosci.* **9,** 639–647
46. Hinkle, C. L., Diestel, S., Lieberman, J., and Maness, P. F. (2006) *J. Neurobiol.* **12,** 1378–1395
47. Covault, J., Merlie, J. P., Goridis, C., and Sanes, J. R. (1986) *J. Cell Biol.* **102,** 731–739